

Supplementary Material

Recovery of superbase ionic liquid using aqueous two-phase systems

Filipe H. B. Sosa¹, Ilkka Kilpeläinen², João Rocha¹ and João A.P. Coutinho^{1*}.

¹CICECO – Aveiro Institute of Materials, Department of Chemistry, University of Aveiro, 3810-193 Aveiro, Portugal

²Department of Chemistry, University of Helsinki, Helsinki, Finland

*Corresponding author: João A. P. Coutinho, E-mail address: jcoutinho@ua.pt

S1 – Tie-lines

$$OF = 10^{10} \sum_{i=1}^N (Y_i^{exp} - Y_i^{mod})^2 \quad (S1)$$

$$Y_T = \left(\frac{Y_M}{\alpha}\right) - \left(\frac{(1-\alpha)}{\alpha}\right) \cdot Y_B \quad (S2)$$

$$Y_T = A \cdot \exp(B \cdot X_T^{0.5} - C \cdot X_T^3) \quad (S3)$$

$$Y_B = A \cdot \exp(B \cdot X_B^{0.5} - C \cdot X_B^3) \quad (S4)$$

$$X_T = \left(\frac{X_M}{\alpha}\right) - \left(\frac{(1-\alpha)}{\alpha}\right) \cdot X_B \quad (S5)$$

M , T , and B denote the mixture, the top phase, and the bottom phase, respectively, X is the weight fraction of salt, Y is the weight fraction of IL, and α is the ratio between the mass of the top phase and the total mass of the mixture.

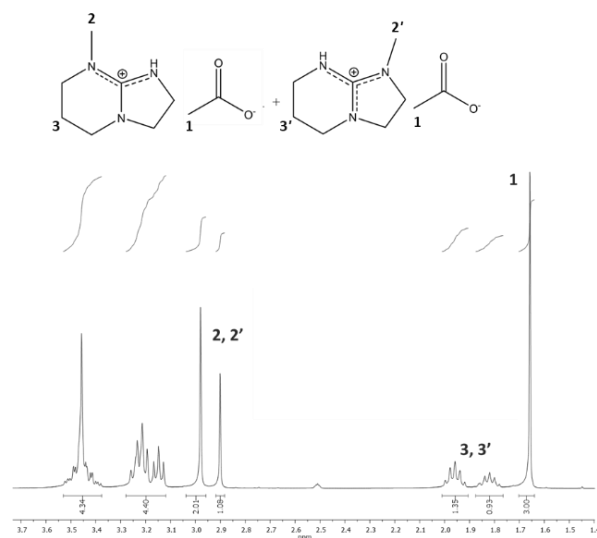


Fig. S1. $^1\text{H-NMR}$ spectra $[\text{mTBNH}][\text{OAc}]$.

S2 – List of tested salts

Table S1. List of tested salts.

Name	Formula
Sodium chloride	NaCl
Potassium chloride	KCl
Caesium chloride	CsCl
Ammonium sulfate	$(\text{NH}_4)_2\text{SO}_4$
Potassium sulfate	K_2SO_4
Copper(II) sulfate	CuSO_4
Manganese sulphate	MnSO_4
Sodium sulfate	Na_2SO_4
Ferrous sulfate (II)	FeSO_4
Magnesium Sulfate	MgSO_4
Zinc sulfate	ZnSO_4
Sodium carbonate	Na_2CO_3
Potassium carbonate	K_2CO_3
Sodium hydrogen carbonate	NaHCO_3
Potassium nitrate	KNO_3
Sodium nitrate	NaNO_3
Ammonium nitrate	NH_4NO_3
Potassium citrate	$\text{C}_6\text{H}_5\text{K}_3\text{O}_7$
Sodium citrate	$\text{Na}_3\text{C}_6\text{H}_5\text{O}_7$
Tri-potassium citrate	$\text{C}_6\text{H}_5\text{K}_3\text{O}_7$
Sodium phosphate dibasic	Na_2HPO_4
Potassium phosphate	K_3PO_4
Diammonium hydrogen phosphate	$(\text{NH}_4)_2\text{HPO}_4$
Sodium dihydrogenphosphate	NaH_2PO_4
Aluminium acetate	$(\text{HO})_2\text{AlCH}_3\text{CO}_2$
Calcium acetate	$\text{C}_4\text{H}_6\text{CaO}_4$
Sodium acetate	$\text{C}_2\text{H}_3\text{NaO}_2$
ammonium peroxodisulfate	$\text{H}_8\text{N}_2\text{O}_8\text{S}_2$
Sodium tartrate	$\text{NaC}_4\text{H}_4\text{O}_6$
Lithium scetate dihydrate	$\text{C}_2\text{H}_3\text{LiO}_2$
Potassium sodium tartrate	$\text{KNaC}_4\text{H}_4\text{O}_6$
Sodium perchlorate	NaClO_4

S3 – Experimental data

Table S2. Experimental binodal curve mass fraction data of K_2CO_3 (1) + [mTBNH][OAc] (2) + water (3) at 298.2 K and 102.8 kPa.

$100w_1$	$100w_2$	$100w_1$	$100w_2$	$100w_1$	$100w_2$
Liquid-liquid equilibrium data					
3.1	66.6	16.3	27.6	28.6	10.9
5.7	53.4	18.7	23.0	30.4	8.8
6.6	50.1	19.1	21.2	33.4	6.4
7.4	48.9	20.4	21.2	35.7	4.8
9.2	42.0	22.4	17.7	38.2	2.3
11.3	37.0	24.1	16.9	42.4	1.3
12.9	33.2	25.4	14.1	45.4	1.3
14.6	28.7	28.6	10.5		

Standard uncertainties u are $u(w_1) = 0.005$, $u(w_2) = 0.005$, $u(T) = 0.5$ K, $u(P) = 10$ kPa.

Table S3. Experimental binodal curve mass fraction data of K_2CO_3 (1) + [mTBNH][OAc] (2) + water (3) at 323.2 K and 102.8 kPa.

$100w_1$	$100w_2$	$100w_1$	$100w_2$	$100w_1$	$100w_2$
Solid-liquid equilibrium data					
1.4	91.2	2.2	82.8	3.1	73.7
Liquid-liquid equilibrium data					
4.6	64.5	15.9	28.5	27.2	10.9
5.1	61.1	18.3	25.1	28.4	10.9
7.6	50.5	19.7	22.8	31.3	8.2
8.3	48.0	21.6	21.0	32.7	6.9
9.7	43.5	22.0	19.5	35.3	5.2
10.6	39.1	23.8	17.1	38.6	3.4
10.9	43.6	24.7	13.9	41.4	2.2
13.0	33.7	26.2	12.1	43.7	4.3
14.7	30.6				

Standard uncertainties u are $u(w_1) = 0.005$, $u(w_2) = 0.005$, $u(T) = 0.5$ K, $u(P) = 10$ kPa.

Table S4. Experimental binodal curve mass fraction data of K_3PO_4 (1) + [mTBNH][OAc] (2) + water (3) at 298.2 K and 102.8 kPa.

$100w_1$	$100w_2$	$100w_1$	$100w_2$	$100w_1$	$100w_2$
Solid-liquid equilibrium data					
1.7	90.4	2.4	73.7		
Liquid-liquid equilibrium data					
3.1	57.0	10.2	24.9	21.8	11.1
4.1	53.2	11.0	23.0	24.3	7.9
4.8	47.6	12.4	20.4	26.2	6.2
6.2	38.6	13.6	21.9	27.3	5.9
6.4	33.7	14.2	20.8	30.1	4.6
7.8	30.8	16.1	15.4	37.0	3.8
8.0	31.4	17.7	16.9	45.0	2.5
9.8	27.8	19.2	12.7		
9.9	27.8	20.1	12.1		

Standard uncertainties u are $u(w_1) = 0.005$, $u(w_2) = 0.005$, $u(T) = 0.5$ K, $u(P) = 10$ kPa.

Table S5. Experimental binodal curve mass fraction data of K_3PO_4 (1) + [mTBNH][OAc] (2) + water (3) at 323.2 K and 102.8 kPa.

$100w_1$	$100w_2$	$100w_1$	$100w_2$	$100w_1$	$100w_2$
Liquid-liquid equilibrium data					
2.9	63.4	8.2	29.7	27.8	5.3
2.4	58.7	10.3	23.3	35.5	3.2
4.1	50.2	13.6	17.7	44.9	2.0
4.4	44.4	19.5	11.1		
5.7	38.8				

Standard uncertainties u are $u(w_1) = 0.005$, $u(w_2) = 0.005$, $u(T) = 0.5$ K, $u(P) = 10$ kPa.

Table S6. Fitted and correlation parameters of Eq. 1 used to describe experimental binodal data for systems at 298.15 K and 102.8 kPa.

System	A	B	C	R ²
K_3PO_4 + [mTBNH][OAc] + H ₂ O	197.24	-0.64	$6.12 \cdot 10^{-7}$	0.99
K_2CO_3 + [mTBNH][OAc] + H ₂ O	124.22	-0.35	$2.53 \cdot 10^{-5}$	0.99

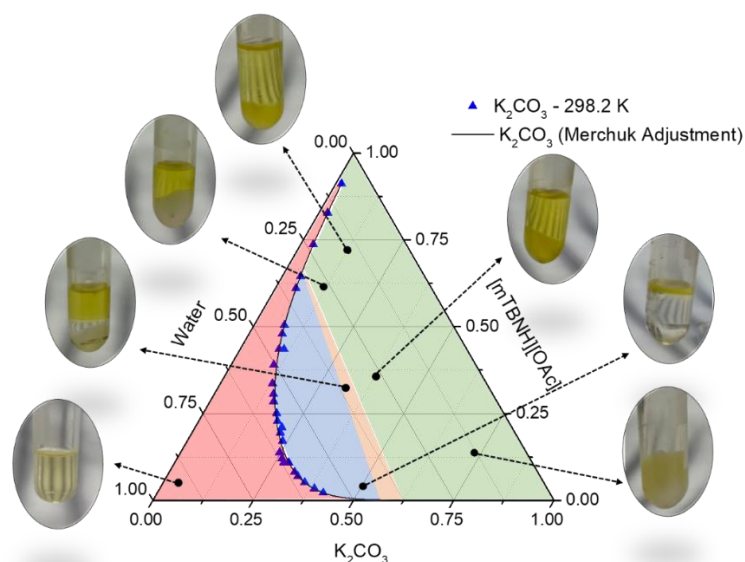


Fig. S2. Representation of the phase diagram of the system composed of K_2CO_3 + $[mTBNH][OAc]$ + H_2O at 323.2 K. The red area corresponds to the homogeneous liquid phase region, the blue area is the liquid-liquid equilibrium region, the orange area is the solid-liquid equilibrium region, and the green area is the solid-liquid region.

Table S7. Comparison between the water composition determined by Merchuk methodology and Karl-Fischer technic for system K_2CO_3 + $[mTBNH][OAc]$ + water and K_3PO_4 + $[mTBNH][OAc]$ + water at 298.2 K and 102.8 kPa.

Tie-Line	Water (wt%) – Merchuk		Water (wt%) - Karl-Fischer	
	Top	Bottom	Top	Bottom
K_2CO_3 + $[mTBNH][OAc]$ +water				
TL2	47.8 %	56.5 %	48.3 %	56.8 %
TL4	38.1 %	51.0 %	38.4 %	51.5 %
TL6	32.3 %	46.0 %	32.6 %	45.8 %
K_3PO_4 + $[mTBNH][OAc]$ +water				
TL2	57.4 %	58.9 %	58.1 %	58.6 %
TL4	45.3 %	48.5 %	44.9 %	48.7 %
TL6	34.2 %	37.5 %	34.4 %	37.4 %

S4 – NRTL

The γ_i of NRTL model, using mass fraction, is calculated as follow:

$$\ln\gamma_i = \frac{\sum_j \frac{\tau_{ji}G_{ji}w_j}{M_j}}{\sum_k \frac{G_{ki}w_k}{M_k}} + \sum_j \left[\frac{w_j G_{ji}}{M_j \sum_k \frac{G_{kj}w_k}{M_k}} \left[\tau_{ij} - \frac{\sum_k \frac{\tau_{kj}G_{kj}w_k}{M_k}}{\sum_k \frac{G_{kj}w_k}{M_k}} \right] \right] \quad (\text{S6})$$

$$\tau_{ij} = \frac{A_{0ij} + A_{1ij}T}{T} \quad (\text{S7})$$

$$G_{ij} = \exp(-\alpha_{ij}\tau_{ij}) \quad (\text{S8})$$

where A_{0ij} and A_{1ij} are the characteristic parameters of energy of the i - j interactions, M_k is the molecular mass of compound k , w_k is the mass fraction of compound k , and parameter α_{ij} is related to the non-randomness of the mixture.

S5- NMR results

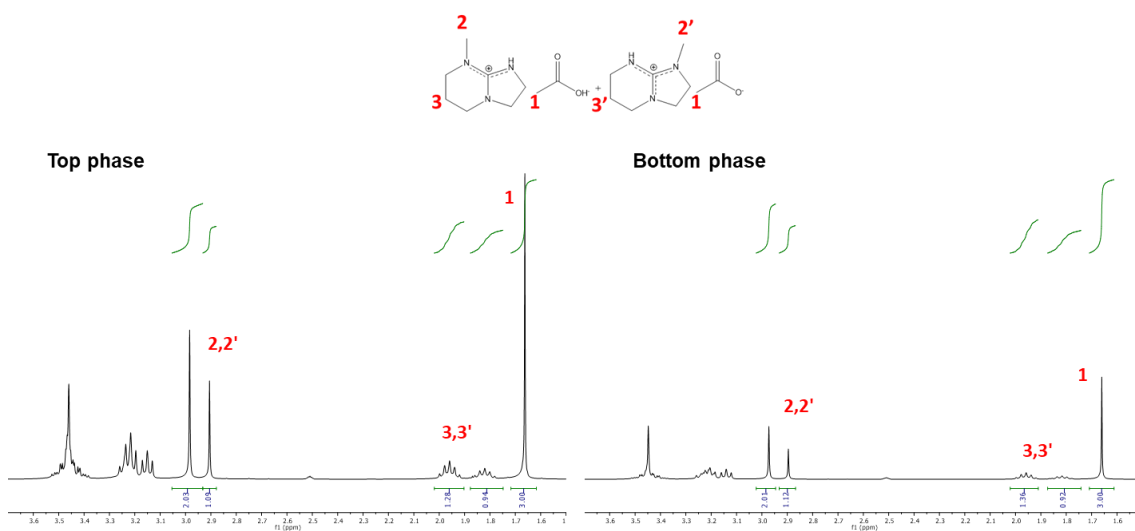


Fig. S3. ¹H-NMR spectra of top phase (right) and bottom phase (left) of TL3 of $\text{K}_2\text{CO}_3 + [\text{mTBNH}][\text{OAc}] + \text{H}_2\text{O}$ system at 298.2 K.

S6- Potassium Removal



Fig. S4. Photo of IL solution with (A) 1.1 wt% K_2CO_3 and (B) 4.6 wt% K_2CO_3 after cellulose dissolution. Condition: 85 wt% [mTBNH][OAc], 7.5 wt% water and 7.5 wt% cellulose at 353.2 K for 24 hours.